PHYSICAL REVIEW C VOLUME 26, NUMBER 4 OCTOBER 1982

Reaction cross sections for $^{14}N+^{14}N$

P. A. DeYoung, J. J. Kolata, L. J. Satkowiak, and M. A. Xapsos
Physics Department, University of Notre Dame, Notre Dame, Indiana 46556
(Received 17 June 1982)

Excitation functions for the yields of eleven residual nuclei from the $^{14}N+^{14}N$ reaction have been measured over the range $E_{c.m.}=7-25$ MeV in steps of ~ 250 keV with γ-ray techniques. The magnitude and energy dependence of the excitation functions for the partial yields are very different from those for the $^{12}C+^{16}O$ system. The total fusion cross section is similar to that from $^{12}C+^{16}O$ when compared at the same center of mass energy, but appears to saturate at an energy and magnitude which are lower than expected from previous systematics. Small, regular fluctuations can be seen in the fusion cross section at the $1-2\%$ level.

[NUCLEAR REACTIONS $^{14}N(^{14}N,x)$; $E_{c.m.}=7-25$ MeV; measured excitation functions for production of $A=16-27$ reaction products; observed small structures at $E_{c.m.}=15.0$, 17.1, 18.5, 20.4, and 22.0 MeV; deduced critical angular momentum for fusion.]

I. INTRODUCTION

The $^{12}C+^{16}O$ system has been found to exhibit resonantlike structure in the total fusion cross section as well as in several of the excitation functions for the production of individual residual nuclei.[1-6] In addition, it has been found that the trajectory of the critical angular momentum deduced from the fusion cross section exhibits similar behavior for a variety of systems.[7] The most notable of these similarities is a sharp break in this trajectory where it intersects the extended ground state band of the compound nucleus, and the association of this break in slope with a characteristic resonantlike structure. In a recent experiment, we have compared the behavior of the critical angular momentum for the $^{16}O+^{16}O$ and the $^{12}C+^{20}Ne$ reactions,[8] both of which form the ^{32}S compound nucleus. These two reactions are simultaneously well matched in excitation energy and angular momentum, and both entrance channels consist of spin-zero alphalike nuclei. Strong similarities were found between the trajectories of the deduced critical angular momentum of the two systems, and a resonantlike structure correlated in both reactions was also identified.

The $^{14}N+^{14}N$ and $^{12}C+^{16}O$ reactions provide an opportunity to compare and contrast the behavior of two very different entrance channels resulting in the same compound system. The $^{14}N+^{14}N$ reaction involves a symmetric system of odd-odd spin-one bosons (nonzero channel spin). In contrast, the asymmetric $^{12}C+^{16}O$ system is composed of alphalike spin-zero nuclei. The former entrance channel also brings 10.6 MeV more energy into the compound system for a given center-of-mass (c.m.) energy. Because the sizes of the nuclei involved are similar, the angular momentum carried in by each entrance channel is approximately the same at a given center-of-mass energy. Consequently, angular momentum and excitation energy cannot simultaneously be matched, so that at equal center-of-mass energies one is populating very different regions in the compound nucleus.

In this work, we present data on the $^{14}N+^{14}N$ reactions comparable to those already obtained[1-6] for the $^{12}C+^{16}O$ system. The behavior of the trajectory of the critical angular momentum for fusion of these two systems was found to be rather different. Possible reasons for these differences will be discussed. In addition, the existence of small, regular fluctuations in the total fusion yield for $^{14}N+^{14}N$ is reported.

II. EXPERIMENTAL METHOD AND RESULTS

The experiment was performed with a ^{14}N beam from the University of Notre Dame three-stage tan-

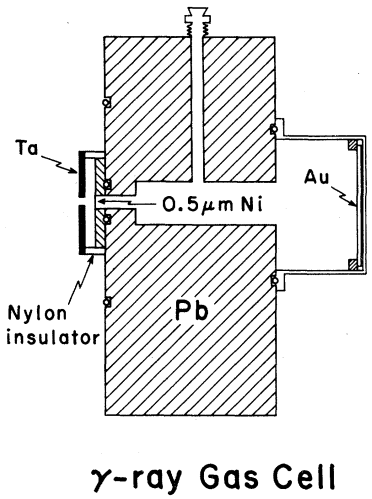

FIG. 1. A cross-sectional view of the gas cell used for this work. The detector was located in a plane perpendicular to the page containing the beam, and placed at an angle of 55° to the beam.

dem Van de Graaff accelerator. The range of beam energies was $E_{lab}=18-52$ MeV, with a step size of 500 keV. The target was typically 50 $\mu g/cm^2$ of ^{14}N, in the form of natural N_2 with an isotopic purity of 99.6%. The gas was contained in a gas cell (Fig. 1) consisting of a bored-out Pb brick, a 450 $\mu g/cm^2$ Ni window to contain the gas at a typical pressure of 30 Torr, and a Au-backed thin-walled Al cylinder which comprised the target volume. The gas continuously flowed through the cell to avoid contamination problems, and the pressure was regulated with a Cartesian-diver manostat.

Gamma rays were detected by a 90 cm^3 Ge(Li) detector placed at 55° with respect to the beam and 7 cm from the target. The detector was shielded from γ rays originating outside the Al cylinder by the Pb body of the cell and, when needed, by additional Pb shielding. The effectiveness of the shielding was checked by removing the gas from the cell at one point during the experiment. With no gas present, only Coulomb excitation of the Au backing was observed. The results of the analysis of this "no-target" γ-ray spectra, using identical spectrum stripping methods as in the "target-in" case, are shown in most of the excitation functions by the data point at $E_{c.m.}=11$ MeV with negligible cross section. The primary relative normalization of the data, which was derived from the 279 and 547 keV transitions in ^{197}Au under the assumption that the Coulomb-excitation cross section is locally smooth, agreed with that obtained from charge collection to within 2% (rms deviation). The long term behavior of the excitation functions was determined from charge collection. As regards both the short and long term behavior, the measured Au Coulomb-excitation yields were found to be in excellent agreement with the predictions of a thick target Winther-de Boer multiple-Coulomb-excitation program.[9] The absolute normalization was determined by measuring the ^{24}Mg yield from the $^{16}O+^{16}O$ reaction at $E_{c.m.}=23.3$ and 19.1 MeV. The $^{16}O+^{16}O$ runs were related to the $^{14}N+^{14}N$ runs through the observed Coulomb-excitation yields. This requires a detailed knowledge of the dependence of the thick target Coulomb-excitation yields on the incident charge (Z), which was measured for several ions and compared to the predictions of the Coulomb excitation program. The agreement between the predictions and experiment was found to be good to approximately 2%, with the remaining discrepancy being ascribed to difficulties in charge collection. Corrections were made to account for the difference in gas pressure between the $^{16}O+^{16}O$ and $^{14}N+^{14}N$ runs, as well as for the efficiency function of the Ge(Li) detector. The estimated uncertainty in the absolute normalization of the total yield is 13%, primarily due to the 7% uncertainty in the absolute normalization of the $^{16}O+^{16}O$ reaction yields.

The ground state transitions which were summed to determine the yields of the various residual nuclei are shown in Table I. In most cases, only the Doppler-shifted component of the line shape has

TABLE I. Ground state γ-ray transitions observed from the $^{14}N+^{14}N$ reaction.

Nuclides	Evaporated particles	E_γ (keV)
^{27}Al	p	844[a], 1014
^{26}Al	pn	417, 830[b], 2511
^{26}Mg	$2p$	1808
^{25}Mg	$2pn$	585[c]
^{23}Na	αp	440, 2640
^{23}Mg	αn	451
^{22}Na	αpn	583[c], 891, 1528
^{22}Ne	$\alpha 2p$	1275
^{20}Ne	2α	1634
^{19}F	$2\alpha p$	197
^{16}O	3α	6130

[a]This transition was unresolved from the 830 keV transition in ^{26}Al and is included in the ^{26}Al excitation function.

[b]$1^+\rightarrow 0^+$ transition to the 228 keV isomeric state.

[c]These transitions were unresolved.

been used in determining the reaction yield, to ensure that there is no contribution from reactions occurring in the body of gas cell (e.g., neutron activation of the Al cylinder). However, for those γ rays resulting from the decay of long-lived states this treatment may result in incorrect yields. Long-lived reaction products formed within the Pb brick may travel into the aluminum cell before decaying, resulting in an increase in the measured yields. Alternately, some of the long-lived reaction products formed within the cell may be stopped in the Au backing before decaying, appearing as narrow, unshifted lines and thus resulting in a decrease in the measured yields. For the $^{14}N + {}^{14}N$ system, these effects are very important for the 197 keV line from ^{19}F and the 583 keV doublet from $^{22}Na + {}^{25}Mg$, for which the lifetimes are so long that essentially all of the residual nuclei, whether formed in the cell or the brick, stop in the backing before decaying. The prompt Doppler-shifted component of the line shape is unobservable for these transitions. It is possible, however, to calculate the fraction of the stopped yield which is due to residual nuclei formed in the volume of the aluminum cell from the angular distributions of the recoil ions (computed by the Monte Carlo evaporation code LILITA),[10] the known lifetimes of the states in question,[11] and the geometry of the gas cell. An estimate of the uncertainty in this calculation has been included in the measured yields of these γ rays.

Excitation functions for the production of ^{27}Al,

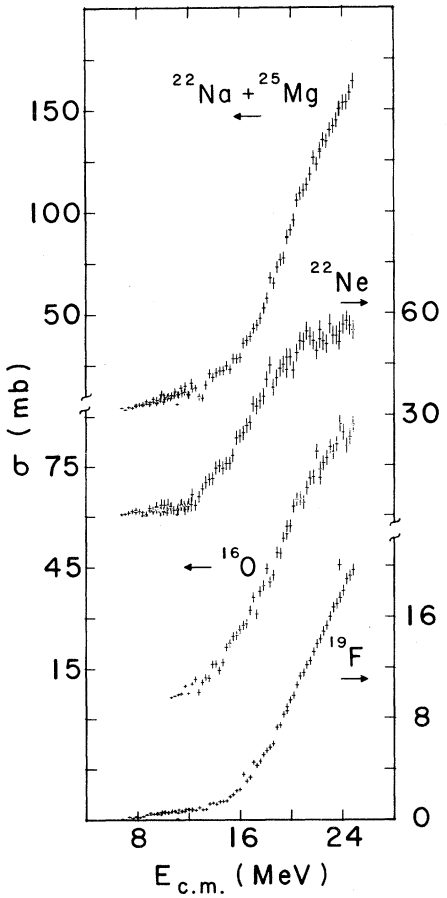

FIG. 2. The excitation functions for the production of $^{22}Na + {}^{25}Mg$, ^{22}Ne, ^{16}O, and ^{19}F measured in the present experiment.

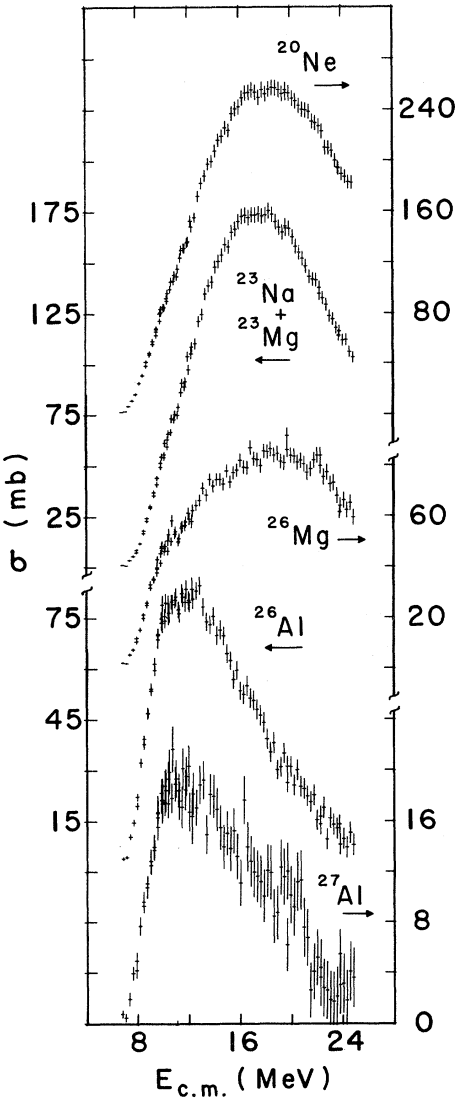

FIG. 3. The excitation functions for the production of ^{27}Al, ^{26}Al, ^{26}Mg, $^{23}Na + {}^{23}Mg$, and ^{20}Ne measured in the present experiment. The 844 keV transition from ^{27}Al has been included with the ^{26}Al yields.

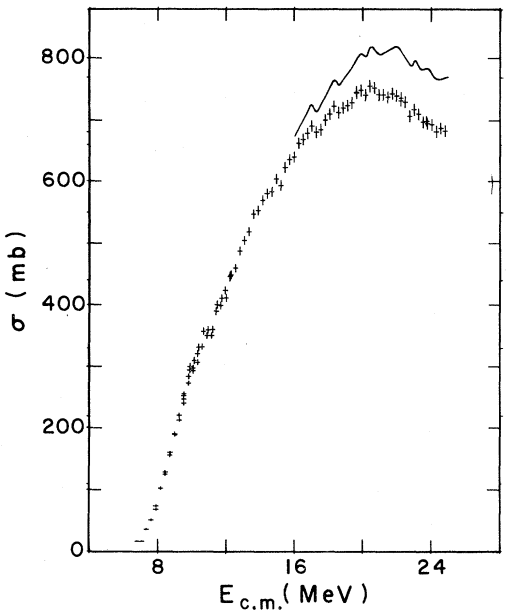

FIG. 4. The excitation function for the total fusion cross section measured in the present experiment. The solid line is the total fusion cross section including an estimate of the yield of the 2^+, 6919 keV transition in ^{16}O.

^{26}Al, ^{26}Mg, $^{22}Na + ^{25}Mg$, $^{23}Na + ^{23}Mg$, ^{22}Ne, ^{20}Ne, ^{19}F, and ^{16}O from the $^{14}N + ^{14}N$ reaction are shown in Figs. 2 and 3. The excitation function for the total fusion yield, which is obtained by summing the individual channels listed above, is shown in Fig. 4. The solid line in this figure is the total fusion cross section obtained by summing the channels listed above and also including an estimate of the yield from the 2^+, 6919 keV state in ^{16}O based on the results of Ref. 12. In each case, the error bars indicated are the statistical uncertainties in the peak areas, added in quadrature to the 2% rms deviation in the relative normalization discussed above. Possible systematic uncertainties include summing effects, which have been found to be negligibly small in the experimental geometry used, and γ-ray angular distribution effects which may be on the order of a few percent for the individual reaction yields. Finally, it should be noted that γ-ray techniques are not sensitive to direct population of the ground state of a residual nucleus. The contribution of ground-state yields to the total fusion cross section is estimated to be approximately 5%.

TABLE II. Comparison of some measured fusion cross sections for $^{14}N+^{14}N$.

$E_{c.m.}$ (MeV)	σ (mb) Present work	σ (mb) Ref. 13
7.0	16.5± 2.1	8.6[a]± 2.6
		8.1[b]± 2.4
8.2	103 ±13	79[b] ± 23.9
9.0	189 ±25	196[a] ± 59
		198[b] ± 59
10.0	297 ±39	329[a] ± 99
		350[b] ±105
11.0	357 ±46	517[a] ±155

[a]Results obtained with a Ge(Li) detector.
[b]Results obtained with a NaI detector.

III. DISCUSSION

A. Comparison with other experiments

Representative values taken from previous low-energy measurements of the $^{14}N + ^{14}N$ fusion cross section by Switkowski *et al.*[13] are compared to the results in this work in Table II. This measurement was performed with a combination of NaI detectors at ±90° and a Ge(Li) detector at 0° with respect to the beam axis. Solid targets consisting of various nitrides were bombarded by a ^{14}N beam over the energy range $4.68 \leq E_{c.m.} \leq 10.99$ MeV. The measured γ-ray yields [discrete γ-ray lines in the Ge(Li) spectra] were corrected by a branching and summing factor calculated under the assumption of a $2J+1$ population of excited states in the residual nuclei. The total γ-ray yields determined from the NaI detectors were normalized to the Ge(Li) results. Only the ^{20}Ne, ^{23}Na, ^{26}Mg, and ^{26}Al exit channels were considered, and only the results for the total fusion cross section were presented. The agreement between the two works is fair: The error bars overlap at all but the lowest common energies. However, the long-term behavior of the fusion cross sections as determined in the two experiments is somewhat different. The fusion cross section measured in this work increases less rapidly than that of Switkowski *et al.* The difference could be due to the assumption of a $2J+1$ population of excited states, or perhaps to the angular distribution of the γ radiation.

Cassagnou *et al.*[14] have also investigated the $^{14}N + ^{14}N$ system with γ-ray techniques. Their energy step size was larger than in the present experiment and only preliminary results have as yet been given. The agreement between these experiments for the most part is very good, with the only areas of disagreement being the identification of certain

TABLE III. Comparison of the maximum cross section for the strongest exit channels for $^{14}N+^{14}N$.

Residual nucleus	σ_{max} (mb) Present work	σ_{max} (mb) Ref. 14
^{20}Ne	250	250
^{26}Al	80	70
$^{23}Na+^{23}Mg$	180	190
$^{22}Na+^{25}Mg$	170	180

γ-ray lines and the behavior of the ^{16}O (3α) and ^{19}F ($2\alpha p$) excitation functions. These latter channels are just opening at the highest energies measured in both experiments. Table III summarizes the measured maximum yield for four major reaction channels from the present work and Ref. 14.

B. Comparison with the $^{12}C+^{16}O$ system

Partially smoothed excitation functions for the measured exit channels from the $^{14}N+^{14}N$ system are compared in Fig. 5 to the results of Chan *et al.*[5] for $^{12}C+^{16}O$, as a function of the center-of-mass energy. Unlike the $^{12}C+^{20}Ne$ and $^{16}O+^{16}O$ systems, which exhibit similar behavior when compared as a function of excitation energy in the compound nucleus,[8] the $^{14}N+^{14}N$ and $^{12}C+^{16}O$ data appear more similar when compared as a function of center-of-mass energy. The excellent agreement between the total fusion excitation functions at the lower energies is taken as an indication that in this energy regime both systems are being limited by the available reaction cross section allowed by the optical-model potential, which is similar for the two reactions.[6,15] However, the magnitude of the maximum total fusion cross section, and the energy where the excitation function appears to saturate, are not as expected. This point will be discussed in more detail below.

The observed differences in the partial yields can be qualitatively understood by consideration of the fact that very different regions of excitation of the compound system are populated by the two entrance channels. At a given center-of-mass energy, which implies similar angular momentum for the

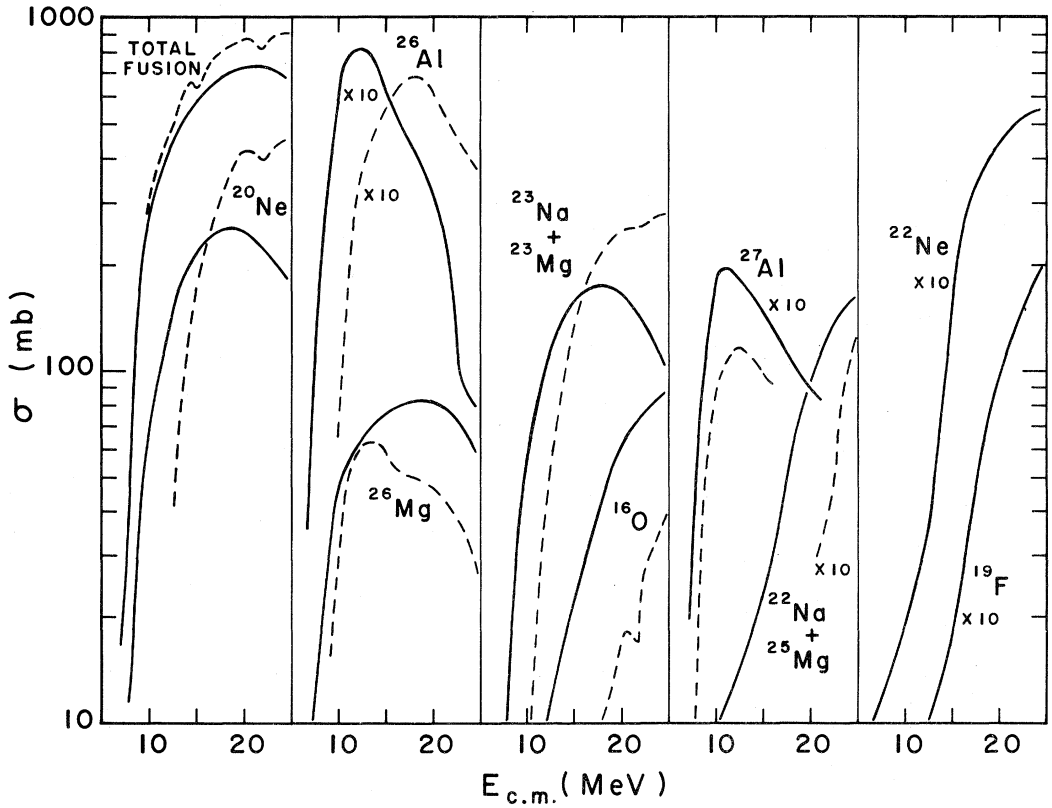

FIG. 5. Partially smoothed excitation functions from the $^{14}N+^{14}N$ system (solid curve) and from the $^{12}C+^{16}O$ system (Ref. 5, dashed curve) compared as a function of the center-of-mass energy.

two systems, the $^{14}N+^{14}N$ entrance channel populates a much higher region of excitation energy in the compound nucleus. The increased amount of energy which must be carried off before the residual nucleus can γ decay results in a tendency toward longer evaporation sequences in the $^{14}N+^{14}N$ system than for $^{12}C+^{16}O$.

C. Trajectory of the critical angular momentum

The critical angular momentum for the fusion of identical spin-one bosons is deduced from the measured fusion cross section, taking into account the channel spin and symmetric nature of the $^{14}N+^{14}N$ system. In this case, all partial waves contribute, though not equally, due to coupling of the orbital angular momentum with the intrinsic spin of the two ^{14}N nuclei. The expression relating the fusion cross section to the critical angular momentum, in the context of the sharp cutoff model, is given by:

$$\sigma_f=\pi\lambda\!\!\!^{-2}\left[\tfrac{4}{3}\sum_{l=\text{even}}^{l_c}(2l+1)+\tfrac{2}{3}\sum_{l=\text{odd}}^{l_c}(2l+1)\right], \tag{1}$$

where $\lambda\!\!\!^{-}$ is the reduced wavelength. As discussed in Ref. 7, the orbital angular momentum is treated as a continuous variable in order to approximately compensate for the use of the sharp cutoff approximation. Unlike the cases presented there, however, the presence of sums over different subsets of l does not readily allow the reduction of this expression to closed form. Thus the critical angular momentum for the $^{14}N+^{14}N$ system was obtained from Eq. (1) by first calculating σ_f as a function of an integral upper limit of the sums. This function was then inverted and l_c was determined by interpolating between the discrete point of the inverted function at the value of the measured fusion cross section. The results of this procedure for the $^{14}N+^{14}N$ fusion cross section (including the estimated yield from the 2^+ state in ^{16}O) are shown in Fig. 6 along with the results from Ref. 7 for the $^{12}C+^{16}O$ system. The 10.6 MeV difference in the Q value between the two entrance channels is immediately obvious. Another difference is that the critical angular momentum trajectory for $^{14}N+^{14}N$ does not follow that deduced from theoretical reaction cross sections calculated from an optical-model potential. The corresponding comparison for $^{12}C+^{16}O$ was rather good.[7] This divergence of the l_c trajectory from that predicted using the Reilly potential[15] may be due to an increased direct reaction strength due to

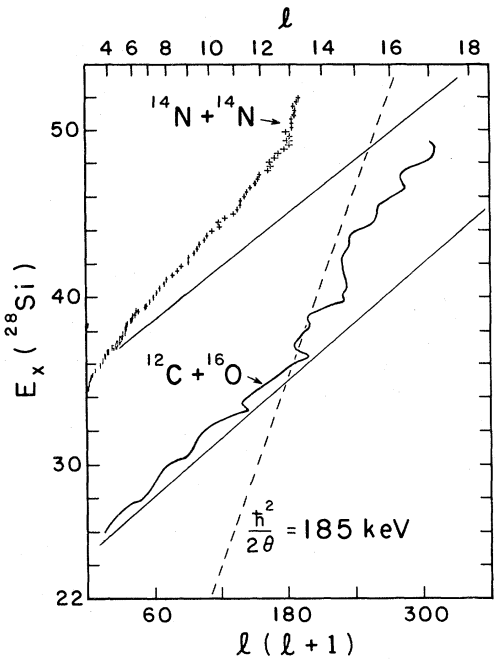

FIG. 6. The critical angular momentum trajectory for $^{14}N+^{14}N$ deduced from the fusion cross section (including an estimated contribution from the 6919 keV transition from ^{16}O). Also shown is the trajectory for $^{12}C+^{16}O$ taken from Ref. 7, the trajectories deduced from the reaction cross section calculated with the potentials of Refs. 6 and 15, and the extended ground state band of ^{28}Si (having moment-of-inertia parameter $\hbar^2/2\theta=185$ keV).

the presence of the four unpaired outer-shell nucleons in the $^{14}N+^{14}N$ system. The greatest difference between the results for the two systems is that saturation of the l_c trajectory for the $^{14}N+^{14}N$ entrance channel occurs at a lower angular momentum, reflecting the fact that the measured fusion cross section saturates at a magnitude and energy which are lower than expected if the limit to fusion is due to properties of the compound system. Similar behavior has been observed in the ^{24}Mg system, where two entrance channels ($^{12}C+^{12}C$ and $^{10}B+^{14}N$) have been studied.[16] The scarcity of data points and possible absolute normalization differences between different experiments renders the interpretation of the excitation functions of the $^{10}B+^{14}N$ fusion cross section somewhat uncertain. However, we note that, above the ^{24}Mg excitation energy at which the $^{14}N+^{10}B$ yield saturates, the critical angular momentum trajectories are separated by approximately four units of angular momentum. Perhaps coincidentally, this equals the differ-

ence between the maximum channel spin of the two entrance channels. In the present experiment, the difference of about $2\hbar$ units of angular momentum at saturation also equals the maximum allowed channel spin. Qualitatively similar dependence of the value of l_c at saturation on the maximum entrance channel spin has been observed for four channels leading to the ^{27}Al compound system.[17] Finally, we note that a recent investigation[18,19] of the ^{23}Na compound system, formed via four different entrance channels, shows evidence for similar effects. In this latter study, the discrepancies with optical-model predictions discussed above also appear in certain of the entrance channels and particularly for $^{14}N+^{9}Be$.

Also of interest is the fact that the $^{14}N+^{14}N$ system shows evidence of regular structure in its total fusion yield. In particular, we note the small vertical segments which occur at excitation energies of 42.2, 44.3, 45.7, 47.6, and 49.2 MeV (corresponding to $l_c=9-13$) in the critical angular momentum plot of Fig. 6. These changes in slope correspond to small fluctuations in the total fusion yield at $E_{c.m.}=15.0$, 17.1, 18.5, 20.4, and 22.0 MeV. A close association between similar structures and integral l_c values has previously been observed for other symmetric systems.[7] However, in these cases the channel spin was zero so that only even l values could contribute to the reaction yield. Thus, although the measured oscillations are quite weak (1–2%), it is probable they represent the first observation of such regular structure in systems with nonzero channel spin. On the other hand, the oscillations do not appear to be related to the gross structures seen in the elastic scattering excitation function,[15] as was the case[20] for $^{16}O+^{16}O$. In particular, we note that the predicted and observed structures in the excitation function are not equally spaced, due to the unequal weighting of even and odd partial waves in the reaction cross section. This is in contrast to the regular spacing of the broad oscillations in the $^{14}N+^{14}N$ elastic scattering cross section.[15]

V. CONCLUSION

Excitation functions for the production of eleven residual nuclei have been measured over the energy range $7 \leq E_{c.m.} \leq 25$ MeV. Comparison of the individual exit channels with previous results for the $^{12}C+^{16}O$ system at similar compound-nuclear excitation energies reveals very little similarity, due to the extremely different regions of excitation energy in the compound nucleus which are populated by the two entrance channels. The excitation functions are more nearly similar when compared at equal center-of-mass energies, approximately corresponding to equivalent angular momentum in the compound system.

The $^{14}N+^{14}N$ fusion cross section is found to be very similar to that for $^{12}C+^{16}O$ at low energies, where each is limited by the available reaction cross section. On the other hand, the saturation of the deduced critical angular momentum for $^{14}N+^{14}N$ is not that expected from compound nuclear limitation models, but rather differs by approximately the maximum available entrance channel spin. Qualitatively similar behavior has been observed in other systems. It may be that this effect, as well as the earlier divergence of the critical angular momentum trajectory from that predicted by the optical model, is due to an increased direct reaction strength due to the presence of four unpaired outer-shell nucleons in the $^{14}N+^{14}N$ system.

Finally, regular (but not equally spaced) oscillations have been observed in the $^{14}N+^{14}N$ total fusion cross section, at energies expected for consecutive integral values of the critical angular momentum. These structures, although very weak in consequence of the large channel spin in this system, nevertheless appear to be related to the similar (but equally-spaced) oscillations in the fusion cross section for symmetric spin-zero boson systems, which have been interpreted as shape resonances in the optical model potential.

This work was supported by the National Science Foundation, under Grant No. PHY-80-08234.

[1]J. J. Kolata, R. M. Freeman, F. Haas, B. Heusch, and A. Gallmann, Phys. Lett. 65B, 333 (1976); Phys. Rev. C 19, 408 (1979).

[2]D. Branford, B. N. Nagorcka, and J. O. Newton, J. Phys. G 3, 1565 (1977).

[3]B. Čujec and C. A. Barnes, Nucl. Phys. A266, 461 (1976).

[4]H. Frölich, P. Dück, W. Galster, W. Treu, H. Voit, H. Witt, W. Kuhn, and S. M. Lee, Phys. Lett. 64B, 408 (1976).

[5]Y. D. Chan, H. Bohn, R. Vandenbosch, K. G. Bernhardt, J. G. Cramer, R. Sielemann, and L. Green, Nucl. Phys. A303, 500 (1978).

[6]P. Sperr, S. Vigdor, Y. Eisen, W. Henning, and D. G.

Kovar, T. R. Ophel, and B. Zeidman, Phys. Rev. Lett. 36, 405 (1976).
[7]J. J. Kolata, Phys. Lett. 95B, 215 (1980).
[8]P. A. DeYoung, J. J. Kolata, R. C. Luhn, R. E. Malmin, and S. N. Tripathi, Phys. Rev. C 25, 1420 (1982).
[9]Program SWHET obtained from Dr. R. O. Sayer, Oak Ridge National Laboratory (unpublished).
[10]Program LILITA obtained from Dr. J. Gomez del Campo, Oak Ridge National Laboratory (unpublished).
[11]R. J. de Meijer, A. G. Drentje, and H. S. Plendl, At. Data Nucl. Data Tables 15, 391 (1975).
[12]J. J. Kolata, R. M. Freeman, F. Haas, B. Heusch, and A. Gallmann, Phys. Rev. C 21, 579 (1980).
[13]Z. E. Switkowski, R. G. Stokstad, and R. M. Wieland, Nucl. Phys. A274, 202 (1976).
[14]Y. Cassagnou, R. Dayras, R. Fonte, G. Lanzano, A. Palmeri, and L. Rodriquez, Saclay Report CEA-N-2207, 1980, p. 38.
[15]W. Reilly, R. Wieland, A. Gobbi, M. W. Sachs, and D. A. Bromley, Il Nuovo Cimento 13A, 897 (1973).
[16]M. E. Ortiz, J. Gomez del Campo, Y. D. Chan, D. E. DiGregorio, J. L. C. Ford, Jr., D. Shapira, R. G. Stokstad, J. P. F. Sellschop, R. L. Parks, and D. Weiser, Phys. Rev. C 25, 1436 (1982).
[17]Y. D. Chan, D. E. DiGregorio, J. L. C. Ford, Jr., J. Gomez del Campo, M. E. Ortiz, and D. Shapira, Phys. Rev. C 25, 1410 (1982).
[18]J. F. Mateja, R. L. Kozub, J. Garman, A. D. Frawley, L. C. Dennis, and K. W. Kemper, Bull. Am. Phys. Soc. 27, 478 (1982).
[19]J. F. Mateja, A. D. Frawley, L. C. Dennis, K. Abdo, and K. W. Kemper, Phys. Rev. C 25, 2963 (1982).
[20]J. J. Kolata, R. M. Freeman, F. Haas, B. Heusch, and A. Gallmann, Phys. Rev. C 19, 2237 (1979).